Brain Topogr (2010) 23:292–300
DOI 10.1007/s10548-010-0144-z

ORIGINAL PAPER

# Variable Anisotropic Brain Electrical Conductivities in Epileptogenic Foci

**M. Akhtari · M. Mandelkern · D. Bui · N. Salamon · H. V. Vinters · G. W. Mathern**

Received: 23 November 2009 / Accepted: 2 April 2010 / Published online: 4 May 2010


**Abstract** Source localization models assume brain electrical conductivities are isotropic at about 0.33 S/m. These assumptions have not been confirmed ex vivo in humans. This study determined bidirectional electrical conductivities from pediatric epilepsy surgery patients. Electrical conductivities perpendicular and parallel to the pial surface of neocortex and subcortical white matter ($n = 15$) were measured using the 4-electrode technique and compared with clinical variables. Mean (±SD) electrical conductivities were $0.10 \pm 0.01$ S/m, and varied by 243% from patient to patient. Perpendicular and parallel conductivities differed by 45%, and the larger values were perpendicular to the pial surface in 47% and parallel in 40% of patients. A perpendicular principal axis was associated with normal, while isotropy and parallel principal axes were linked with epileptogenic lesions by MRI. Electrical conductivities were decreased in patients with cortical dysplasia compared with non-dysplasia etiologies. The electrical conductivity values of freshly excised human brain tissues were approximately 30% of assumed values, varied by over 200% from patient to patient, and had erratic anisotropic and isotropic shapes if the MRI showed a lesion. Understanding brain electrical conductivity and ways to non-invasively measure them are probably necessary to enhance the ability to localize EEG sources from epilepsy surgery patients.

**Keywords** Seizure · Epilepsy · Surgery · Pediatric · Anisotropic · EEG · MEG · Source localization model

M. Akhtari · D. Bui
Neuropsychiatric Institutes, David Geffen School of Medicine, University of California, Los Angeles, CA, USA

M. Akhtari
Department of Physics and Astronomy, The University of New Mexico, Albuquerque, NM, USA

G. W. Mathern
Department of Neurosurgery, The Intellectual and Developmental Disabilities Research Center, and The Brain Research Institute, David Geffen School of Medicine, University of California, Los Angeles, CA, USA

H. V. Vinters
Departments of Pathology and Laboratory Medicine and Neurology, David Geffen School of Medicine, University of California, Los Angeles, CA, USA

M. Mandelkern
Department of Physics, University of California, Irvine, CA, USA

N. Salamon
Department of Radiology, David Geffen School of Medicine, University of California, Los Angeles, CA, USA

M. Akhtari (✉)
760 Westwood Plaza, Rm C8-836, Los Angeles, CA 90015, USA
e-mail: Akhtarim@ucla.edu

## Introduction

*M*agneto*E*ncephalo*G*raphy (MEG), *E*lectro*E*ncephalo*G*raphy (EEG) and combined MEG–EEG are techniques for localization of intracranial interictal and ictal current sources and areas of neuronal activation (Ebersole 1999; Jun et al. 2008). To localize intracranial EEG and MEG data, mathematical models have been developed which rely on assumptions regarding electrical conductivity through the skull and brain.

The model of the volume conductor affects localization accuracy in MEG and EEG signals (Gencer and Acar 2004;

Hamalainen and Sarvas 1989; Wen and Li 2001). Volume conductor models assume that the human cranium consists of brain (white matter and cortex), CSF, skull, and scalp. Knowledge of tissue conductivities (termed $\sigma$, inverse of resistivities $\rho$) are necessary to reduce errors in calculating the forward solution of the extracranial magnetic fields and electric potentials produced by intracranial sources. Misspecification of tissue conductivities can affect the apparent magnitude (strength) of magnetic fields and electric surface potentials (Awada et al. 1998; Haueisen et al. 2002; Okada et al. 1999) leading to source miss-localization in simmulation (Marin et al. 1998; Pohlmeier et al. 1997; Van Uitert et al. 2004), and experimental studies (Akhtari et al. 2002a). Although information of the conductivity ratio of adjacent compartments may be sufficient in some models, knowledge of electrical conductivities are needed for finite element and combination MEG/EEG models (Law 1993; Haueisen et al. 1997).

Misspecification of brain electrical conductivity could contribute to error in calculations of the electromagnetic forward solutions and source localization (Vatta et al. 2002; Bruno et al. 2002; Fuchs et al. 1998a, b). Most source localization models use a nominal isotropic value of 0.33 S/m for conductivity of the brain volume (Gutierrez et al. 2004). This is based on brain tissue from normal autopsy cases after long post-mortem delays, and has not been measured immediately *ex vivo* in patients with epileptogenic lesions (Gabriel 2005; Schmid et al. 2003a).

This study measured electrical conductivities parallel and perpendicular to the pial surface in freshly excised brain tissues obtained from epilepsy surgery patients. Our goal was to determine if bidirectional electrical conductivities were isotropic and uniform as assumed by source localization models or vary from patient to patient with anisotropic shapes depending on the epileptogenic lesion.

## Methods

### Patient Selection

The cohort consisted of patients with intractable epilepsy who underwent resective neurosurgery at the University of California, Los Angeles (UCLA) Pediatric Epilepsy Surgery program from June 2007 to September 2009. This study was approved by the Institutional Review Board, and patients and their families signed research informed consents and ascents, and HIPAA authorization. Inclusion criteria was if the planned cortical resection was large enough that additional brain tissue beyond what was needed for diagnostic histopathology would be available for research. Except for the size of the operation there were no exclusion criteria.

Clinical data was abstracted from the medical record for comparison with brain electrical conductivities (Lerner et al. 2009). This included side of the operation (right, left), gender (Male, Female), history of infantile spasms, surgery type (hemispherectomy, focal/lobar resections), age at seizure onset, age at surgery, and number of anti-epilepsy drugs (AED) taken at the time of surgery. Epilepsy duration was calculated as the time, in years, from the age at seizure onset to age at surgery. Seizure frequency was calculated as seizures per day based on the number of events captured during inpatient video/EEG telemetry. Etiology was classified as cortical dysplasia (CD) using the Palmini classification system (Palmini et al. 2004) and included the single case of tuberous sclerosis complex (TSC). Non-CD consisted of patients with a history of perinatal infarcts and infections, Rasmussen encephalitis, low grade tumors, Sturge-Weber syndrome, and mesial temporal lobe epilepsy from hippocampal sclerosis (HS) (Salamon et al. 2008). Areas sampled for electrical conductivities were assessed semi-quantitatively by the MRI into cortical regions that were nearly normal (Score 1), partly abnormal with slightly altered cortical anatomy on T1 imaging and slight increase in white matter T2 signal (Score 2), and severely abnormal with grossly abnormal cortical surfaces and increased T2 signal in the gray and white matter (Score 3; Fig. 1). MR images were acquired on a 1.5-T Siemens Sonata scanner (Siemens Medical Systems, South Iselin, NJ). The structural MRI protocol included T1 sagittal (TR/TE 400/14, matrix 256 × 192, 5 mm thickness), 3D T1 coronal Magnetization Prepared Rapid Gradient Echo sequence (MPRAGE) (TR/TE 25/9, TI 8, matrix 256 × 256, 1.8 mm thickness), T2 axial (TR/TE 3000/80, matrix 256 × 192, 4 mm thickness), FLAIR axial (TR/TE 8000/108, TI 2000, matrix 256 × 192, 4 mm thickness), FLAIR coronal (TR/TE 8000/18, matrix 256 × 192, 4 mm thickness), and T2 coronal (TR/TE 4000/85, matrix 256 × 192, 4 mm thickness). MRI scans were interpreted by a neuroradiologist (N.S.) for signs of abnormal cortical development or other etiologies.

### Brain Sample Site Selection and Preparation

At surgery, sample sites were chosen so that the tissue blocks would contain roughly equal portions of gray and subcortical white matter with orientation of the pial surface clearly visible. Sites were chosen from the lateral cortical surface involving the crown of a gyrus, and one site per patient was used for conductivity studies. When possible, sample areas were those least involved with the underlying epileptogenic lesion by MRI, but this varied from case to case (see Fig. 1). From the larger freshly delivered surgical specimen, blocks of cerebral cortex and underlying white matter measuring approximately 12 mm in width, length

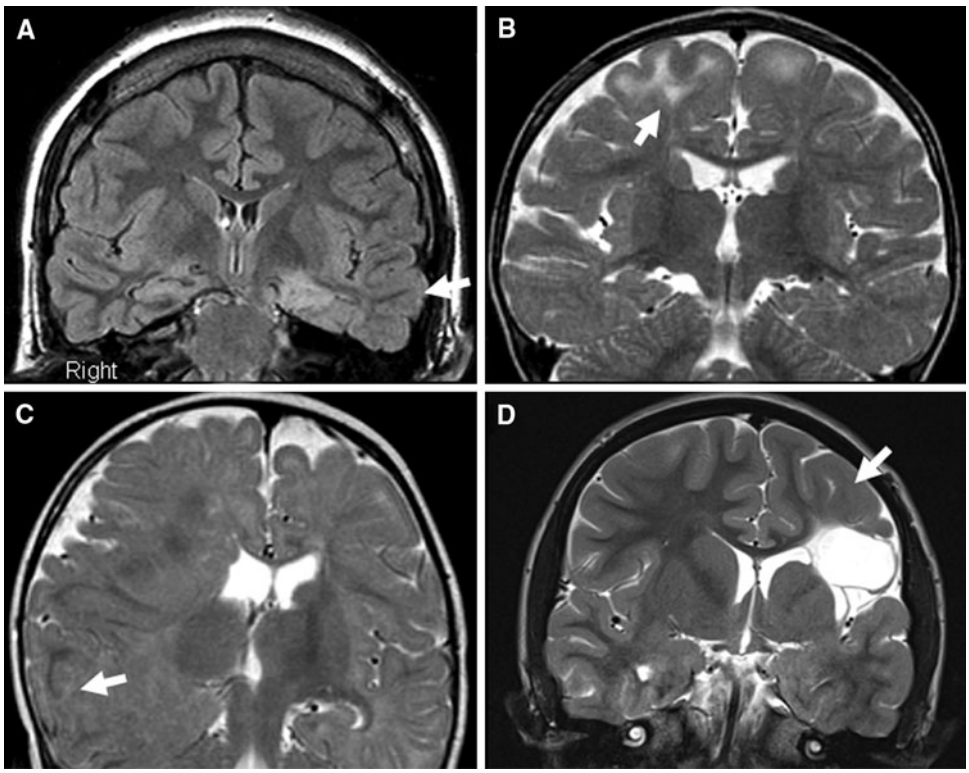


**Fig. 1** Illustration of location of tissue sample sites by MRI. **a** This 20 year old (Case #1; Table 1) had left mesial temporal mild cortical dysplasia and mesial temporal lobe epilepsy. The tissue sample site for electrical conductivity was the middle temporal gyrus, which was near normal by MRI criteria (*white arrow*; MRI Score 1). The percent change was +25% indicating an anisotropic shape with the long axis perpendicular to the pial surface. **b** This 1.6 year old (Case #8; Table 1) had tuberous sclerosis complex (TSC). The sample site was the right frontal tuber (*white arrow*; MRI Score 2; moderately abnormal) which showed −2%, which is essentially isotropic. **c** This 1.5 years old (Case #14; Table 1) had severe cortical dysplasia and subcortical heterotopic lesions. The brain sample site was the right temporal cortex (*white arrow*; MRI Score 3; severely abnormal). The electrical conductivity measurements showed a percent change of −20% indicating an anisotropic shape with the long axis parallel to the pial surface. **d** This 9 year old (Case #15; Table 1) had a perinatal infarct in the left prefrontal branch of the middle cerebral artery. The sample site was the left middle frontal gyrus which was adjacent to the area of damage and abnormal by MRI (*white arrow*; MRI Score 3; severely abnormal). The electrical conductivity measurements showed a percent change of −20% indicating an anisotropic shape with the long axis parallel to the pial surface

and depth were cut with a #10 blade and immediately prepared for conductivity studies. The remainder of the surgical specimen was given to the neuropathologist for histopathology. Sample sites came from temporal, parietal, and frontal regions of the brain. After surgery, the surgeon noted the location of the sample site relative to the MRI scan in the operative notes.

A non-conductive plastic syringe (12 mm diameter) was cut on both ends to obtain an empty cylinder. Holes (5 mm apart, 0.5 mm diameter) were drilled in the middle of this cylinder. Two silver coated copper wires (0.3 mm diameter) were secured 5 mm apart with epoxy glue on a non-conducting piece of Plexiglas. The sample end of wires was 6 mm long with 4 mm exposed. Circular indium foil pieces were cut to cover the surface of the rubber tips of two syringe plungers. Silver wires were attached to the bottom surface of the indium foil which was then glued to the rubber tip. The wire was routed out through small holes in the rubber tip and the plastic housing of the plunger.

The brain tissue sample was placed inside the cylinder symmetrically with respect to the holes and the plungers were placed on either side. The sample was oriented so that the gray matter was at one end and the subcortical white matter was at the other end of the cylinder. This orientation measured electrical conductivities perpendicular to the pial surface. The same procedure was repeated with the sample rotated by 90 degrees with only white matter exposed to the wires within the measurement holes. This measurement was parallel to the pial surface through the subcortical white matter. Experiments were performed immediately after tissue was excised in the operating room.

## Brain Electrical Conductivity

Measurements of brain electrical conductivities *ex vivo* were similar to a previous publication by our group, and used the four-electrode method (Schwan 1968; Akhtari et al. 2006). The current is passed through the sample using

two electrodes, and the potential drops across the sample are measured using a separate pair of electrodes. This method eliminates problems associated with contact impedance.

A function generator (Stanford Research Systems, SR360) was used to modulate the current output of a linear stimulus isolator (World Precision Instruments, A350) at several frequency settings (Fig. 2). A resistor (505 Ω) was placed in series with the brain tissue samples. The potential drop across this resistor was measured with a lock-in-amplifier (Stanford Research Systems, SR830 DSP Lock-in Amplifier) to obtain the applied current passing through the sample and the phase of the potential (outside the sample) with respect to the modulation signal of the function generator. The potential drop across lead wires and the phase between this potential and applied current were measured with a second identical lock-in amplifier. LabView software (LabView, National Instruments) was written to control the function generator and the lock-in amplifiers

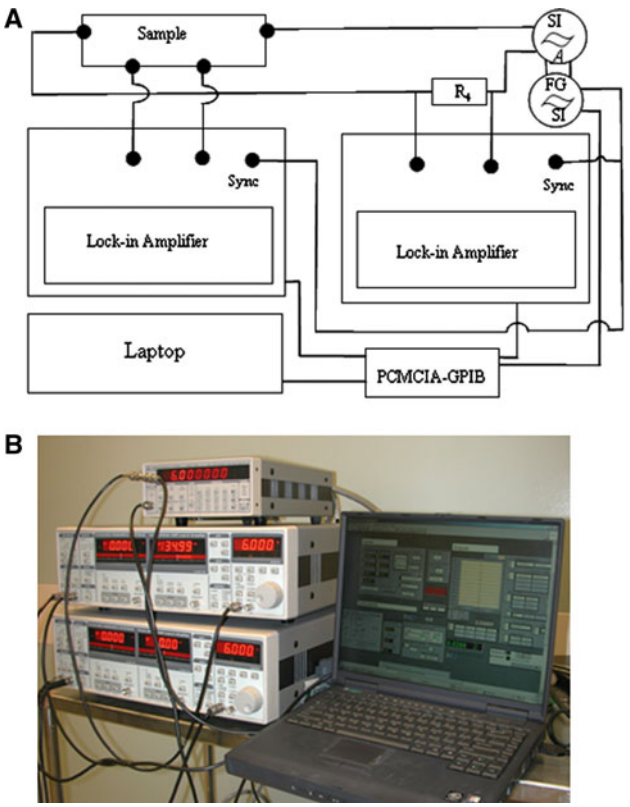


**Fig. 2** Schematic diagram of the conductivity measuring instrumentation. **a** A function generator (FG) is used to modulate the current output of a stimulus isolator (SI) through the sample. The potential drops and phase changes are measured through the lock-in amplifiers. The resistor $R_4$ is used to monitor the current and the phase change due to instrumentation. All instrumentation is automated through LabView software and controlled through the laptop computer, which also records and analyzes all data. **b** Photograph of the instrumentation in the operating room

through GPIB card (PCMCIA-GPIB, National Instruments). This software was also used to acquire data, which were stored in a laptop computer (Gateway Solo 9300, Gateway Inc.). The absolute phase change across the sample was obtained by subtracting the phase angles measured with the first and second lock-in amplifiers, respectively. The frequency of the applied current was varied from 6 to 96 Hz in steps of 10 Hz and from 105 to 1005 Hz in steps of 100 Hz. Each set of data was obtained at current amplitude of 60 μA. The overall errors in potential and phase measurements were determined by replacing the sample with a known resistor (R = 988 Ω) and a R||C circuit respectively (Akhtari et al. 2003).

The lead separation inside the cylinder was determined using a digital caliper (0.03 mm precision). The areas of the top and bottom surfaces of each sample were determined by measuring the areas of the indium electrodes that covered the respective surfaces. Therefore, the curvatures of the surfaces of the plunger were automatically considered in area measurements. The lower bound of uncertainty (i.e. due to instrumentation) in conductivity measurements was calculated using

$$\delta\sigma = \left[\left(\left(\frac{\partial\sigma}{\partial l}\right)\delta l\right)^2 + \left(\left(\frac{\partial\sigma}{\partial A}\right)\delta A\right)^2 + (\delta R)^2 + (\delta S)^2\right]^{1/2}$$

where $l \equiv$ inter-electrode distance, $A \equiv$ electrode area, $\delta R \equiv$ uncertainty in potential measurement, and $\delta S \equiv$ uncertainty in current measurements, with latter two adjusted for conformity of units. It is noted that $\delta l$ is systematic within the repeated measurements of one sample, while $\delta A$ is systematic within all measurements in all samples. The following SI units and definitions are used throughout this manuscript.

$$\text{Conductance} = \frac{1}{\text{Resistance (R)}},\ \text{unit} \equiv \text{siemens (S)} = \frac{1}{\text{ohm } (\Omega)}$$

$$\text{Conductivity } (\sigma) = \frac{1}{\text{Resistivity } (\rho)},\ \text{unit} \equiv \frac{\text{S}}{\text{meter (m)}}$$

Ohms law, $\sigma = \frac{I}{V}\cdot\frac{l}{A}$, where $I \equiv$ current, $V \equiv$ voltage, $l \equiv$ distance between measuring electrodes, $A \equiv$ surface area of current delivery electrodes, was used to measure conductivity.

## Data Analysis

The electrical conductivities and clinical variables were entered into a database and analyzed using a statistical program (StateView 5; SAS Institute, Inc., Cary NC). The difference of conductivities perpendicular and parallel to the pial surface was calculated as the percent change using

the formula (((Conductivity Perpendicular ($\delta\sigma_{\perp}$) − Conductivity Parallel ($\delta\sigma_{||}$))/$\delta\sigma_{\perp}$)) × 100). To determine if the electrical conductivities perpendicular and parallel to the pial surface were statistically different indicating isotropy or anisotropy, Z scores were calculated using propagated uncertainties (i.e. $(\delta\sigma_{||}^2 + \delta\sigma_{\perp}^2)^{1/2}$) and *P*-values calculated from the Z scores (Table 1). We used uncertainties in determining the presence of anisotropy to account for variability from instrumentation (Akhtari et al. 2006). Other statistical tests included t-tests and ANOVA where appropriate. A priori, results were considered different at a minimal level of significance of $P < 0.05$.

## Results

### RC Circuit-Control Studies

The maximum discrepancies between the experimental and theoretical values of impedance and phase in $R_1 - (R_2||C)$ measurements were 2.6 and 5.4%, respectively. The maximum discrepancies between the experimental and calibrated measurement values of resistance were less than 0.5%. The measured phase values using the $R_3$ resistor deviated from zero degree by less 0.1 degree. These values represent excellent agreement indicating appropriate functions of the instrumentation.

### Cohort Characteristics

The cohort consisted of 15 epilepsy surgery patients (Table 1). Seven (47%) were left sided resections, seven (47%) were female, six (40%) had a history of infantile spasms, and ten (67%) underwent cerebral hemispherectomy while the others had lobar/focal resections. Mean (year ± SD) age at seizure onset was 3.4 ± 4.3, age at surgery was 7.9 ± 6.0, and epilepsy duration was 4.5 ± 4.8. Five cases (33%) were classified as having cortical dysplasia (CD; two Type II, two Type I, and one case of tuberous sclerosis complex). The ten non-CD etiologies consisted of four cases of perinatal infarcts, two cases of Rasmussen encephalitis (RE), and one each of bacterial infection, low grade tumor (ganglioglioma), Sturge-Weber syndrome, and mesial temporal lobe

**Table 1** Cohort clinical information and electrical conductivity perpendicular and parallel to the pial surface

| Case # | Side | Sex | H/O IS | Sz onset | Age Surg. | Epil. Dur. | Surg. type | Etiology category | Etiology type | Sz Freq. | AED | MRI | Cond. Perp. | Cond. Par. | % Diff. | *P*-value |
|---|---|---|---|---|---|---|---|---|---|---|---|---|---|---|---|---|
| 1 | L | M | No | 0.5 | 20.1 | 19.6 | L | CD/T | CD I | 0.33 | 3 | 1 | 10.8 | 8.0 | 25.3 | <0.0001 |
| 2 | L | M | Yes | 7.0 | 9.3 | 2.3 | H | nCD | Infarct | 0.67 | 3 | 1 | 15.4 | 11.7 | 23.9 | <0.0001 |
| 3 | L | F | Yes | 0.1 | 2.8 | 2.72 | H | nCD | Infection | 10 | 2 | 2 | 10.9 | 9.1 | 16.8 | <0.0001 |
| 4 | L | F | Yes | 0.02 | 0.6 | 0.58 | H | CT/T | CD II | 10 | 3 | 2 | 13.7 | 11.9 | 13.4 | <0.0001 |
| 5 | R | M | No | 8.0 | 10.1 | 2.1 | H | nCD | RE | 10 | 2 | 2 | 12.8 | 11.2 | 12.4 | <0.0001 |
| 6 | L | M | No | 2.5 | 10.0 | 7.5 | H | nCD | RE | 6 | 3 | 2 | 11.7 | 11.0 | 5.6 | =0.002 |
| 7 | R | M | Yes | 0.0 | 1.5 | 1.5 | H | nCD | Infarct | 20 | 2 | 2 | 10.4 | 9.9 | 5.0 | =0.001 |
| 8 | Ri | M | Yes | 0.25 | 1.6 | 1.35 | L | CD/T | TSC | 5 | 3 | 2 | 9.8 | 9.9 | −2.2 | =0.271 |
| 9 | R | F | No | 4.0 | 11.0 | 7.0 | L | nCD | Tumor | 1 | 3 | 1 | 10.5 | 10.8 | −3.1 | =0.113 |
| 10 | R | F | No | 12.0 | 16.2 | 4.2 | L | CD/T | CD I | 0.75 | 3 | 2 | 6.3 | 6.7 | −6.8 | =0.031 |
| 11 | L | F | No | 0.12 | 8.3 | 8.12 | H | nCD | Infarct | 1 | 2 | 2 | 9.6 | 10.3 | −7.5 | =0.001 |
| 12 | R | F | No | 0.42 | 2.6 | 2.18 | H | nCD | St. Weber | 10 | 2 | 3 | 9.8 | 11.6 | −18.3 | <0.0001 |
| 13 | Ri | M | No | 12.0 | 14.4 | 2.4 | L | nCD | HS | 0.28 | 1 | 2 | 10.3 | 12.2 | −18.4 | <0.0001 |
| 14 | R | M | Yes | 0.50 | 1.5 | 1.0 | H | CT/T | CD II | 5 | 1 | 3 | 8.0 | 9.6 | −19.6 | <0.0001 |
| 15 | L | F | No | 4.0 | 9.0 | 5.0 | H | nCD | Infarct | 1 | 2 | 3 | 10.0 | 11.9 | −19.7 | =0.0007 |

Cases are stratified by the percent difference in electrical conductivity going from most normal to abnormal

Side is right (R) or left (L) cerebral hemisphere. H/O IS, history of infantile spasms. M, Male. F, Female. Sz Onset, seizure onset in years. Age Surg., age at surgery in years. Epil. Dur., epilepsy duration in years. Surg. Type, surgery type defined as hemispherectomy (H) or lobar (L) resection. Etiology defined as cortical dysplasia/TSC (CD/T), and non cortical dysplasia (nCD). Etiology types include cortical dysplasia Type I (CD I) and Type II (CD II), tuberous sclerosis complex (TSC), Rasmussen encephalitis (RE), hippocampal sclerosis (HS), and Sturge-Weber syndrome (St. Weber). Sz. Freq., seizure frequency per day. AEDs, number of anti-epilepsy durgs presurgery. Cond. Perp., electrical conductivity (S/m × $10^{-2}$) perpendicular (vertical) to the pial surface. Cond. Par., electrical conductivity (S/m × $10^{-2}$) parallel (horizontal) to the pial surface. % Diff., is percent difference between the two conductivity measurements. Positive % Diff. is anisotropic with the long axis perpendicular to the pial surface (greater vertical than horizontal; Cases 1–7), values close to zero are isotropic (equal vertical and horizontal to the pial surface; Cases 8 and 9), and negative values are anisotropic with the long axis parallel (horizontal) to the pial surface; Cases 10–15). *P*-value are t-tests of the mean (±SD) conductivity perpendicular compared with parallel. MRI score is 1 (normal), 2 (mildly abnormal) and 3 (severely abnormal)

epilepsy from hippocampal sclerosis (HS). Presurgery seizure frequency averaged 5.4 ± 5.7 seizures per day, and the number of presurgery anti-epilepsy drugs (AED) per patient was 2.3 ± 0.7. Brain sample sites were considered by MRI to be normal (Score 1) in three patients, slightly abnormal (Score 2) in nine cases, and severely abnormal (Score 3) in three cases. Depending on the planned surgical resection and extent of histopathology, by MRI sample sites used for brain electrical conductivity could be distant to the lesion in relatively normal cortex (Fig. 1a), within the epileptogenic lesion (Fig. 1b, c) or directly adjacent to the lesion in abnormal cortex (Fig. 1d).

## Bidirectional Electrical Conductivities

The average electrical conductivities perpendicular (Cond. Perp.) and parallel (Cond. Par.) to the pial surface varied by 243% from one patient to another (Table 1). Average (±SD) electrical conductivities were 0.10 ± 0.01 S/m which was 30% of the assumed value used in many EEG source models (see Introduction). Averaged together, conductivities perpendicular to the pial surface (0.107 ± 0.021 S/m; range 0.063–0.154) did not differ from values parallel to the pial surface (0.104 ± 0.016 S/m; range 0.067–0.122; $P = 0.708$).

There were differences as to which axis relative to the pial surface had higher conductivities, and whether conductivities were isotropic or anisotropic. This was reflected in the percent change calculation comparing the perpendicular and parallel conductivities. These varied by 45% (+25.3% to −19.7%; Table 1). Positive percent change indicates anisotropic shapes with the long axis perpendicular (vertical) to the pial surface, values near zero indicate isotropic conductivities, and negative percent change indicates anisotropic shapes with the long axis parallel (horizontal) to the pial surface (see ovals at the top of Fig. 3a). Anisotropy in the perpendicular orientation was observed in seven (47%) patients (Table 1; Cases 1–7; $P < 0.002$), isotropic shapes were seen in two patients (13%; Cases 7 and 8), and anisotropy with a parallel orientation was seen in six (40%) patients (Cases 10–15; $P < 0.031$). Hence, anisotropic brain electrical conductivities were noted in 87% of epilepsy surgery patients in this cohort but with different orientations of the long axis.

Percent change positively correlated with electrical conductivities perpendicular (Fig. 3a; $P = 0.0069$) but not parallel (Fig. 3b; $P = 0.496$) to the pial surface. Comparing the two axes, this indicates that the major variability in electrical conductivities were vertical to the pial surface. In addition, the alternations in the percent changes inversely correlated with tissue abnormality using the semi-quantitative MRI scores ($R = -0.721$; $P = 0.0024$; Fig. 1). Anisotropic shapes with the long axis perpendicular to the pial surface were noted in more normal areas by MRI, isotrophic values in partially abnormal regions, and anisotropic with the long axis parallel to the pial surface in mostly abnormal MRI regions. Hence, higher brain electrical conductivities were observed in the vertical direction relative to the pial surface in specimens from most normal areas on MRI. Lower vertical electrical conductivities with isotropic and horizontal anisotropic shapes were most often seen in areas of abnormal MRI findings.

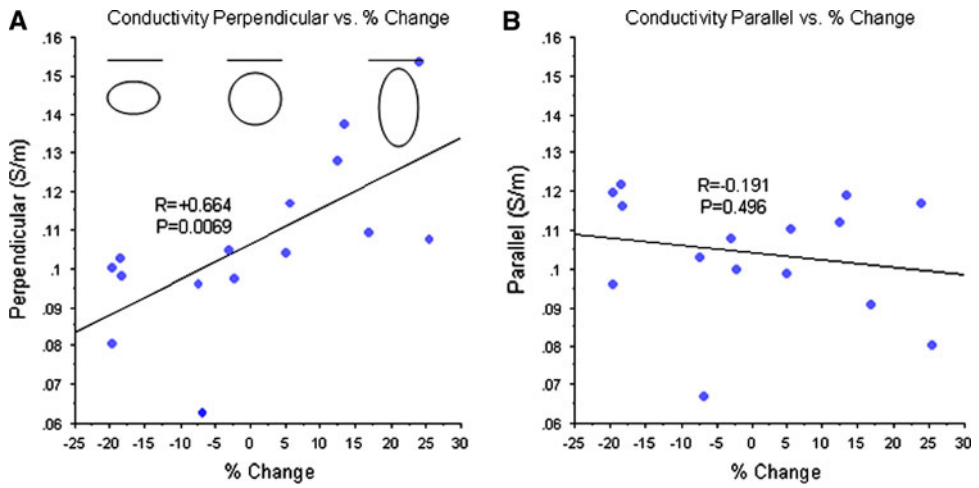


**Fig. 3** Line graphs showing the relationship between the percent change in electrical conductivity by axis (calculated as (((Cond. Perp. − Cond. Par.)/Cond. Perp.)) × 100)) compared with conductivity velocities perpendicular (**a**) and parallel (**b**) to the pial surface by patient. Conductivities perpendicular (vertical) to the pial surface positively correlated with percent change ($P = 0.0069$) while conductivities parallel (horizontal) to the pial surface did not ($P = 0.496$). The changes in electrical conductivities relative to axis direction are illustrated in the oval shapes at the top of (**a**) (line above ovals represents the pial surface). Negative percent change indicate greater anisotropic shapes with the main axis horizontal to the pial surface, values near zero indicate isotropic shapes, and positive percent changes reflect anisotropic shapes with the main axis and vertical to the pial surface

**Table 2** Correlations between clinical values and electrical conductivity measurements

| Clinical variable (ANOVA or t-tests) | Conductivity perpendicular | Conductivity parallel | Percent difference |
|---|---|---|---|
| Side | $P = 0.077$ | $P = 0.701$ | $P = 0.067$ |
| Sex | $P = 0.389$ | $P = 0.899$ | $P = 0.369$ |
| H/O IS | $P = 0.323$ | $P = 0.932$ | $P = 0.259$ |
| Seizure onset | $P = 0.788$ | $P = 0.986$ | $P = 0.598$ |
| Age surgery | $P = 0.683$ | $P = 0.275$ | $P = 0.608$ |
| Epilepsy duration | $P = 0.788$ | $P = 0.161$ | $P = 0.255$ |
| Surgery type | $P = 0.683$ | $P = 0.275$ | $P = 0.608$ |
| Etiology category | $P = 0.250$ | $\mathbf{P = 0.038}$ | $P = 0.796$ |
| Seizure frequency | $P = 0.573$ | $P = 0.796$ | $P = 0.540$ |
| AEDs | $P = 0.295$ | $P = 0.405$ | $P = 0.068$ |

Data presented as *P*-values. Significant differences indicated in Bold type. Abbreviations as in Table 1

### Correlation of Electrical Conductivities and Clinical Variables

With one exception, there were no correlations comparing brain electrical conductivities perpendicular and parallel to the pial surface and percent differences with the clinical factors used in this study (Table 2). The exception was that electrical conductivities horizontal to the brain surface were lower in patients with cortical dysplasia (CD; $0.92 \pm 0.02$ S/m) compared with non-CD etiologies ($0.110 \pm 0.01$ S/m; $P = 0.038$). This is a similar finding as previously reported by our group (Akhtari et al. 2006).

Histopathologic analysis from three subjects showed nearly normal cortical tissue. The mean values of conductivities in these subjects did not show a significant difference compared with other subjects whose histology showed abnormalities (unpaired two-tailed; $P > 0.60$ for both directions).

## Discussion

This study found that bidirectional measures of electrical conductivity through cerebral cortex and subcortical white matter was highly variable in pediatric epilepsy surgery patients. Average electrical conductivities were 30% of the assumed value used for many mathematical models of EEG source localization, and varied by 243% from patient to patient. Brain samples showed anisotropic conductivities whose principal axes (greater values) were perpendicular in 47% and horizontal to the pial surface in 40% of patients (Table 1 and Fig. 1). Percent changes in anisotropy varied by 45% from the highest to lowest values, and were most pronounced perpendicular (vertical) compared with parallel (horizontal) to the pial surface (Fig. 3). Perpendicular principal axes were associated with normal cortex by MRI, while isotropy and parallel principal axes were linked to abnormal cortical regions by neuroimaging. Electrical conductivities were lower in patients with cortical dysplasia compared with non-dysplasia etiologies (Table 2).

These findings are important for models of source localization because human brain electrical conductivities were less than assumed values, and differ significantly from patient to patient with variable anisotropic and isotropic shapes depending on the type and proximity to the MRI lesion. Understanding brain electrical conductivity and ways to measure them with non-invasive methods, such as diffusion tensor imaging, quantitative magnetization transfer, multiple T2 measurements, could enhance the ability to localize EEG and other relevant electrical information in the treatment of epilepsy surgery patients (Widjaja and Raybaud 2008; Basser and Pierpaoli 1996; Beaulieu 2002; Sun et al. 2006). It is important to emphasize that our measurements involved portions of cerebral cortex in or near epileptogenic lesions which is clinically relevant particularly when localization of deeper epileptogenic sources are needed (Marin et al. 1998; Pohlmeier et al. 1997; Van Uitert et al. 2004; Law 1993; Vatta et al. 2002; Gutierrez et al. 2004; Ollikainen et al. 1999; Rullmann et al. 2009).

The patients in this study had epileptogenic etiologies, and areas measured often contained these lesions by MRI. The involvement of abnormal brain tissue is one explanation for the varied isotropic and anisotropic conductivities. Brain tissue components thought to affect electrical conductivities include the orientation of myelin containing membranes in the white matter, density and orientation of neuronal filaments in the gray matter, and astrocyte proliferation (Basser and Pierpaoli 1996; Beaulieu 2002). Which of these components contribute most directly to altered

brain electrical conductivities along with differences in histopathology will be the focus of future studies by our group. In addition, conductivity values varied by about two fold in direction across white matter tracts and about 2.5-fold in the direction of tracts (Sekino et al. 2004). The conductivity values were in the lower range and sometimes below the lowest values reported by other investigators not using fresh brain tissue (Gabriel 2005; Schmid et al. 2003a, b; Gabriel et al. 1996; Geddes and Baker 1967). The variation of tissue conductivity and its corresponding anisotropy, especially in the vicinity of the epileptogenic lesions, suggests that inclusion of accurate conductivity values for individual patients, and not nominal or average values, are necessary when these values are needed for accurate characterization (i.e. orientation, amplitude, or location) of intracranial sources of activity (Vatta et al. 2002; Hallez et al. 2008; Bénar and Gotman 2002; Wolters et al. 2004). How much these variations of electrical conductivities contribute to source miss-localization in humans with epileptogenic foci will require further study, and should be performed in human experimental settings. Based on the results of a previous and current study, we found an average of $0.106 \pm 0.025$ S/m in line with white matter tracts and an average of $0.101 \pm 0.017$ S/m that crossed white matter tracts for brain conductivity (Akhtari et al. 2006). These values may be more realistic in computation of the forward solution, but do not account for the considerable variability from patient to patient observed in our study.

Since significant phase difference was not observed between the measured voltage drop and the applied current, it does not appear necessary to include reactance (capacitance or inductance) in modeling of cerebral cortical tissues. The frequencies used in this study were in the range of the frequencies of interest in EEG and MEG brain activity. The ohmic response of the brain samples indicates that polarization and capacitive effects of brain tissues may be ignored in volume conductor models.

Previous studies by Zhang et al. (2006) and Lai et al. (2005) using in vivo techniques reported brain-to-skull conductivity ratios of $18.7 \pm 1.2$, using realistic head model, and $25 \pm 7$, using 3-spherical shell model, respectively. In these two studies, the scalp potentials were generated through electrodes in subdural grids in epilepsy patients. Conductivity ratio of brain-to-skull obtained through direct *ex-vivo* measurements of freshly excised samples (Akhtari et al. 2002b, 2006) as well as those in this report, show a value of $9.53 \pm 0.29$. Zhang et al. (2006) reported the effect of realistic head model and the grid implant on the estimates of conductivity ratios. The effect of operative skull and scalp defects, on scalp potential distribution due to intracranial sources of activity (Bénar and Gotman 2002) can confound the in vivo conductivity-ratio measurements. The effects of grid implant, such as edema, contusion, or bruising, on brain tissues can also confound these measurements. The effects of these limitations on *ex-vivo* and in vivo conductivity measurements warrant further investigation.

The reader should be aware of potential confounds and experimental limitations when interpreting our study. For example, our measurements were performed *ex vivo* in pediatric patients at operating room temperatures (22°C). Although the conductivity values at body temperature might be systematically higher by 2–3% per degree centigrade (for CSF and muscle tissues, respectively) (Baumann et al. 1997), this does not effect the interpatient variation of conductivity observed in our study. We do not know, however, what might happen to brain electrical conductivities if they were measured in vivo with tissue having active blood circulation or in adult patients. In addition, varying percentages of white and gray matter were present in samples used in our studies. Furthermore, we measured from a single sample per patient, which included different brain lobes. Future studies may need to sample from more than one site per patient to confirm the variability of brain electrical conductivity within subjects. This may have added variability to our measures, but such sampling represents what occurs in clinical practice. Despite these issues, this study found that electrical conductivities in the human brain are variable by direction and by underlying etiology in refractory epilepsy patients undergoing surgery, which may impact EEG source localization techniques.

**Acknowledgements** The authors would like to thank Mr. Maurizio DiMauro (The University of New Mexico, Department of Physics) for his valued contributions. This study was supported by NIH grants R21 NS060675, and R01 NS38992 to GWM and MA. HVV supported in part by the Daljit S. and Elaine Sarkaria Chair in Diagnostic Medicine.



## References

Akhtari M, Bryant H, Flynn E, Lopez N, Padilla R, Merrifield W, Mamelak A, Sutherling W (2002a) MEG, EEG source localization and conductivities of the live human skull. In: BIOMAG 2002, 13th international conference on biomagnetism, Jena, Germany, August 2002

Akhtari M, Bryant HC, Mamelak AN, Flynn ER, Heller L, Shih JJ, Mandelkern M, Matlachov A, Ranken DM, Best ED, DiMauro MA, Lee RR, Sutherling WW (2002b) Conductivities of three-layer live human skull. Brain Topogr 14(3):151–167

Akhtari M, Bryant HC, Emin D et al (2003) A model for frequency dependence of conductivities of the live human skull. Brain Topogr 16(1):39–55

Akhtari M, Salamon N, Duncan R, Fried I, Mathern GW (2006) Electrical conductivities of the freshly excised cerebral cortex in epilepsy surgery patients; correlation with pathology, seizure duration, and diffusion tensor imaging. Brain Topogr 18(4): 281–290

Awada KA, Jackson DR, Baumann SB et al (1998) Effect of conductivity uncertainties and modeling errors on EEG source localization using a 2-D model. IEEE Trans Biomed Eng 45(9):1135–1145

Basser PJ, Pierpaoli C (1996) Microstructural and physiological features of tissues elucidated by quantitative-diffusion-tensor MRI. J Magn Reson B 111(3):209–219

Baumann SB, Wozny DR, Kelly SK, Meno FM (1997) The electrical conductivity of human cerebrospinal fluid at body temperature. IEEE Trans Biomed Eng 44(3):220–223

Beaulieu C (2002) The basis of anisotropic water diffusion in the nervous system—a technical review. NMR Biomed 15(7–8):435–455

Bénar CG, Gotman J (2002) Modeling of post-surgical brain and skull defects in the EEG inverse problem with the boundary element method. Clin Neurophysiol 113(1):48–56

Bruno P, Vatta F, Inchingolo P (2002) Lesion type misidentification: EEG potential sampling and source reconstruction errors. Biomed Sci Instrum 38:435–440

Ebersole JS (1999) Non-invasive pre-surgical evaluation with EEG/MEG source analysis. Electroencephalogr Clin Neurophysiol Suppl 50:167–174

Fuchs M, Wagner M, Wischmann HA et al (1998a) Improving source reconstructions by combining bioelectric and biomagnetic data. Electroencephalogr Clin Neurophysiol 107(2):93–111

Fuchs M, Drenckhahn R, Wischmann HA, Wagner M (1998b) An improved boundary element method for realistic volume-conductor modeling. IEEE Trans Biomed Eng 45(8):980–997

Gabriel C (2005) Dielectric properties of biological tissue: variation with age. Bioelectromagnetics Suppl 7:S12–S18

Gabriel C, Gabriel S, Corthout E (1996) The dielectric properties of biological tissues: I. Literature survey. Phys Med Biol 41(11):2231–2249

Geddes LA, Baker LE (1967) The specific resistance of biological material—a compendium of data for the biomedical engineer and physiologist. Med Biol Eng 5(3):271–293

Gencer NG, Acar CE (2004) Sensitivity of EEG and MEG measurements to tissue conductivity. Phys Med Biol 49(5):701–717

Gutierrez D, Nehorai A, Muravchik CH (2004) Estimating brain conductivities and dipole source signals with EEG arrays. IEEE Trans Biomed Eng 51(12):2113–2122

Hallez H, Vanrumste B, Van Hese P, Delputte S, Lemahieu I (2008) Dipole estimation errors due to differences in modeling anisotropic conductivities in realistic head models for EEG source analysis. Phys Med Biol 53(7):1877–1894

Hamalainen MS, Sarvas J (1989) Realistic conductivity geometry model of the human head for interpretation of neuromagnetic data. IEEE Trans Biomed Eng 36(2):165–171

Haueisen J, Ramon C, Eiselt M, Brauer H, Nowak H (1997) Influence of tissue resistivities on neuromagnetic fields and electric potentials studied with a finite element model of the head. IEEE Trans Biomed Eng 44(8):727–735

Haueisen J, Tuch DS, Ramon C et al (2002) The influence of brain tissue anisotropy on human EEG and MEG. Neuroimage 15(1):159–166

Jun SC, George JS, Kim W et al (2008) Bayesian brain source imaging based on combined MEG/EEG and fMRI using MCMC. Neuroimage 40(4):1581–1594

Lai Y, van Drongelen W, Ding L, Hecox KE, Towle VL, Frim DM, He B (2005) Estimation of in vivo human brain-to-skull conductivity ratio from simultaneous extra- and intra-cranial electrical potential recordings. Clin Neurophysiol 116:456–465

Law SK (1993) Thickness and resistivity variations over the upper surface of the human skull. Brain Topogr 6(2):99–109

Lerner JT, Salamon N, Hauptman JS et al (2009) Assessment and surgical outcomes for mild type I and severe type II cortical dysplasia: a critical review and the UCLA experience. Epilepsia 50(6):1310–1335

Marin G, Guerin C, Baillet S, Garnero L, Meunier G (1998) Influence of skull anisotropy for the forward and inverse problem in EEG: simulation studies using FEM on realistic head models. Hum Brain Mapp 6(4):250–269

Okada YC, Lahteenmaki A, Xu C (1999) Experimental analysis of distortion of magnetoencephalography signals by the skull. Clin Neurophysiol 110(2):230–238

Ollikainen JO, Vauhkonen M, Karjalainen PA, Kaipio JP (1999) Effects of local skull inhomogeneities on EEG source estimation. Med Eng Phys 21(3):143–154

Palmini A, Najm I, Avanzini G et al (2004) Terminology and classification of the cortical dysplasias. Neurology 62(6 Suppl 3): S2–S8

Pohlmeier R, Buchner H, Knoll G et al (1997) The influence of skull-conductivity misspecification on inverse source localization in realistically shaped finite element head models. Brain Topogr 9(3):157–162

Rullmann M, Anwander A, Dannhauer M et al (2009) EEG source analysis of epileptiform activity using a 1 mm anisotropic hexahedra finite element head model. Neuroimage 44(2):399–410

Salamon N, Kung J, Shaw SJ et al (2008) FDG-PET/MRI coregistration improves detection of cortical dysplasia in patients with epilepsy. Neurology 71(20):1594–1601

Schmid G, Neubauer G, Mazal PR (2003a) Dielectric properties of human brain tissue measured less than 10 h postmortem at frequencies from 800 to 2450 MHz. Bioelectromagnetics 24(6):423–430

Schmid G, Neubauer G, Illievich UM, Alesch F (2003b) Dielectric properties of porcine brain tissue in the transition from life to death at frequencies from 800 to 1900 MHz. Bioelectromagnetics 24(6):413–422

Schwan HP (1968) Electrode polarization impedance and measurements in biological materials. Ann NY Acad Sci 148(1):191–209

Sekino M, Inoue Y, Ueno S (2004) Magnetic resonance imaging of mean values and anisotropy of electrical conductivity in the human brain. Neurol Clin Neurophysiol 2004:55

Sun SW, Liang HF, Trinkaus K et al (2006) Noninvasive detection of cuprizone induced axonal damage and demyelination in the mouse corpus callosum. Magn Reson Med 55(2):302–308

Van Uitert R, Johnson C, Zhukov L (2004) Influence of head tissue conductivity in forward and inverse magnetoencephalographic simulations using realistic head models. IEEE Trans Biomed Eng 51(12):2129–2137

Vatta F, Bruno P, Inchingolo P (2002) Improving lesion conductivity estimate by means of EEG source localization sensitivity to model parameter. J Clin Neurophysiol 19(1):1–15

Wen P, Li Y (2001) Comparison study of different head model structures with homogeneous/inhomogeneous conductivity. Australas Phys Eng Sci Med 24(1):31–36

Widjaja E, Raybaud C (2008) Advances in neuroimaging in patients with epilepsy. Neurosurg Focus 25(3):E3

Wolters CH, Anwander A, Maess B, Macleod RS, Friederici AD (2004) The influence of volume conduction effects on the EEG/MEG reconstruction of the sources of the Early Left Anterior Negativity. Conf Proc IEEE Eng Med Biol Soc 5:3569–3572

Zhang Y, van Drongelen W, He B (2006) Estimation of in vivo human brain-to-skull conductivity ratio in humans. Appl Phys Lett 89(22):223903–2239033